

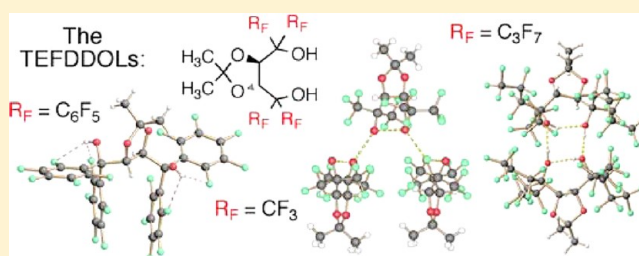
TEFDDOLs ($\alpha,\alpha,\alpha',\alpha'$ -Tetrakis(perfluoroaryl/alkyl)-2,2'-dimethyl-1,3-dioxolane-4,5-dimethanols): Highly Fluorinated Chiral H-Bond Donors and Brønsted Acids with Distinct H-Bonding Patterns and Supramolecular Architectures

Albrecht Berkessel,* Sonja S. Vormittag, Nils E. Schlörer, and Jörg-M. Neudörfl

Department of Chemistry (Organic Chemistry), University of Cologne, Greinstraße 4, 50939 Cologne, Germany

S Supporting Information

ABSTRACT: The synthesis of six enantiopure $\alpha,\alpha,\alpha',\alpha'$ -tetrakis(perfluoroalkyl/aryl)-2,2'-dimethyl-1,3-dioxolane-4,5-dimethanols (TEFDDOLs), by addition of perfluorinated organolithium reagents or Ruppert's reagent (TMS-CF₃) to isopropylidene tartaric dichloride, is reported. X-ray crystal structures of the TEFDDOLs alone or in complexes with H-bond acceptors such as water and DABCO revealed that this new class of highly fluorinated chiral 1,4-diols forms distinct intra- and intermolecular H-bond patterns. Intramolecular OH–OH bonding accounts for the relatively high acidity of the perfluoroalkyl TEFDDOLs (pK_a in DMSO: tetrakis-CF₃, 5.7; tetrakis-C₂F₅, 2.4). For the tetrakis(perfluorophenyl) TEFDDOL, a quite unusual “pseudo-anti” conformation of the diol, with no intramolecular (and no intermolecular) OH–OH bonds, was found both in the crystal and in solution (DOSY and NOESY NMR). The latter conformation results from a total of four intramolecular OH–F_{aryl} hydrogen bonds overriding OH–OH bonding. Due to their H-bonding properties, the TEFDDOLs are promising new building blocks for supramolecular and potentially catalytic applications.



1. INTRODUCTION

In recent years, selective hydrogen bonding has been recognized as one of the most important principles in (asymmetric) organocatalysis.¹ The most broadly applicable hydrogen bond donor motifs are (thio)ureas **1**² and more recently squaramides **2**³ and TADDOLs⁴ **3** (Figure 1). Whereas (thio)ureas and squaramides are typically able to donate two H bonds to a suitable acceptor, TADDOLs—with only few exceptions—typically form one intramolecular and one intermolecular hydrogen bond.⁵ As a consequence, the

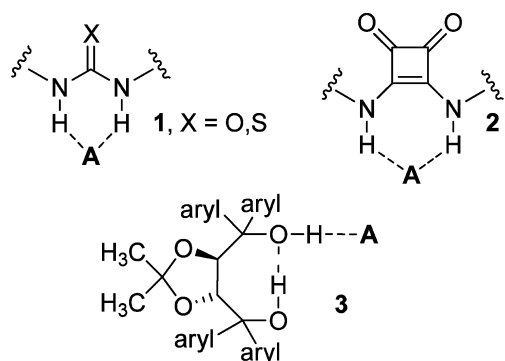


Figure 1. Typical H-bond donor patterns of (thio)ureas **1**, squaramides **2** and TADDOLs **3**. TADDOL = $\alpha,\alpha,\alpha',\alpha'$ -tetraaryl-2,2'-dimethyl-1,3-dioxolane-4,5-dimethanol; A = H-bond acceptor.

intermolecular H-bond donor ability and Brønsted acidity of TADDOLs is enhanced.⁶

On the other hand, fluorinated alcohols such as 1,1,1,3,3,3-hexafluoro-2-propanol (“hexafluoro-*iso*-propanol” (HFIP; **4**), Figure 2) have served in numerous instances as solvents with remarkable properties.⁷ For example, their high solvation power, together with low nucleophilicity, allowed the generation and observation of reactive cationic or radical-cationic species.⁸ Additionally, fluorination accounts for their increased acidity, relative to nonfluorinated analogues.⁷ Not surprisingly, they are good H-bond donors and poor acceptors. Fluorinated alcohols as solvents furthermore promote the epoxidation of olefins and the sulfoxidation of thioethers with hydrogen peroxide.⁹ A recent study of ours established accelerations (of epoxidation) up to 100 000-fold, relative to conventional solvents such as 1,4-dioxane.¹⁰

Altogether, we settled on compound **5a** (Figure 2) as a fluoro alcohol (here HFIP)–TADDOL hybrid. In analogy to the TADDOLs, we dubbed the $\alpha,\alpha,\alpha',\alpha'$ -tetrakis(perfluoroalkyl/aryl)-2,2'-dimethyl-1,3-dioxolane-4,5-dimethanols **5** “TEFDDOLs”. In this article, we describe (i) the synthesis of the hitherto unknown tetrakis(perfluoroalkyl) TEFDDOLs (CF₃ (**5a**), C₂F₅ (**5b**), *n*-C₃F₇ (**5c**), *n*-C₄F₉ (**5d**), *n*-C₆F₁₃ (**5e**); Figure 2), (ii) an improved synthesis of

Received: August 22, 2012

Published: October 2, 2012

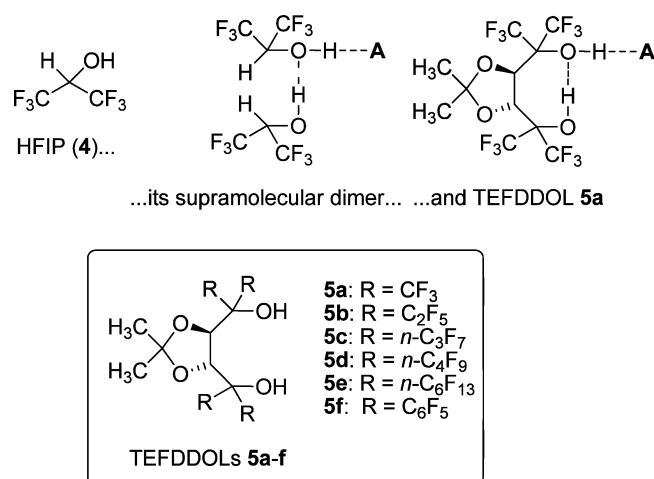


Figure 2. (top) TEFDDOL 5a as a covalent and chiral analogue of a supramolecular HFIP (4) dimer (A = H-bond acceptor). (bottom) TEFDDOLs 5a–f reported in this article.

the tetrakis(pentafluorophenyl) TEFDDOL 5f, (iii) X-ray crystal structures of all TEFDDOLs made and of H-bonded aggregates thereof with H-bond acceptors such as water and amines, and (iv) NMR studies (DOSY) showing that the dimerization of TEFDDOLs by H bonding (as observed in the crystal) persists in solution. It is furthermore shown by NOESY NMR that the quite unusual “pseudoanti” conformation found for 5f in the crystal persists in solution. pK_a values for the TEFDDOLs 5a,b,f have been reported from this laboratory earlier,¹¹ revealing inter alia the remarkably high acidity of the “parent” tetrakis-CF₃ TEFDDOL 5a (pK_a (DMSO) = 5.7) and in particular of its C₂F₅ homologue 5b (pK_a (DMSO) = 2.4). These data suggest that TEFDDOLs may not only be suitable as hydrogen bond donors but may also have potential as chiral Brønsted acid organocatalysts.¹²

Similar to the synthesis of the TADDOLs 3 by Seebach et al.,^{5a} we envisaged the addition of (perfluoroalkyl)lithium reagents¹³ to activated forms (ester, acid chloride) of isopropylidene tartaric acid as the most straightforward approach to the TEFDDOLs 5b–f. An exception is the tetrakis(trifluoromethyl) TEFDDOL 5a, as it is known that (trifluoromethyl)lithium is too unstable to serve as a CF₃ nucleophile.¹³ In this particular case, Ruppert’s reagent (CF₃-TMS, 6) was considered as an alternative CF₃ donor.¹⁴ Before our study, the only TEFDDOL known in the literature was the tetrakis(pentafluorophenyl) TADDOL 5f (Figure 2), reported by Hafner, Duthaler et al.¹⁵ In our hands, however, the procedure by Hafner, Duthaler et al. (employing tartaric ester) gave yields <10% at best. As described in detail below, a quite satisfactory yield of 70% resulted upon switching to the acid chloride as electrophile and in situ quenching.¹⁶

2. RESULTS AND DISCUSSION

2.1. Syntheses. For the tartaric acid electrophiles, we found in extensive optimization studies (not reported) that (*R,R*)-isopropylidene tartaric acid dichloride (7) invariably gave superior yields of TEFDDOLs in comparison to e.g. tartaric esters. This starting material 7 was prepared from (*R,R*)-isopropylidene tartaric disodium salt according to Klotz et al.¹⁷ Upon sublimation, material suitable for X-ray crystallography was obtained. The X-ray crystal structure of 7 is shown in Figure 3.

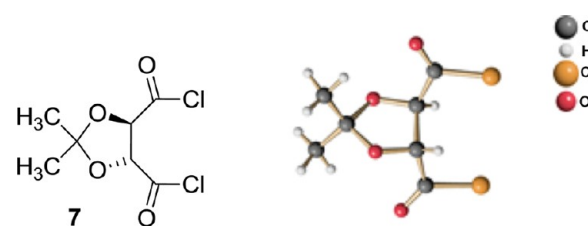
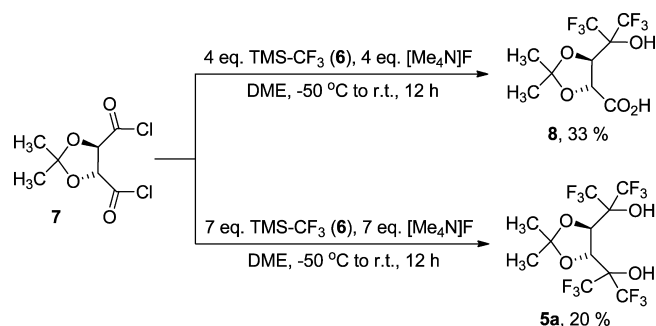


Figure 3. X-ray crystal structure of (*R,R*)-isopropylidene tartaric acid dichloride (7).

2.1.1. Synthesis of the TEFDDOL 5a Using Ruppert’s Reagent (6). When the acid chloride 7 was treated with increasing amounts of Ruppert’s reagent 6 and tetramethylammonium fluoride¹⁸ at –50 °C in DME, significant conversion was observed beginning from ca. 4 equiv of reagent and fluoride used. The trifluoromethylation product 8 was isolated in 33% yield after aqueous workup which, however, turned out not to be the desired TEFDDOL 5a. As evidenced by NMR and in particular by X-ray crystallography, the “semitrifluoromethylated” tartaric acid 8 was formed under these conditions (Scheme 1, top). To our delight, increasing the amount of TMS-CF₃ (6) to ca. 7 equiv resulted in the formation of the TEFDDOL 5a, which could be isolated in 20% yield (Scheme 1, bottom).

Scheme 1. Trifluoromethylation of Isopropylidene Tartaric Acid Dichloride (7), Using Ruppert’s Reagent (6)



The X-ray crystal structures of the tartaric acid bis-(trifluoromethyl) derivative 8 and of the tetrakis-(trifluoromethyl) TEFDDOL 5a are shown in Figure 4. The water-free crystals needed for the X-ray structural analysis of pure 5a were obtained by sublimation under vacuum in a sealed

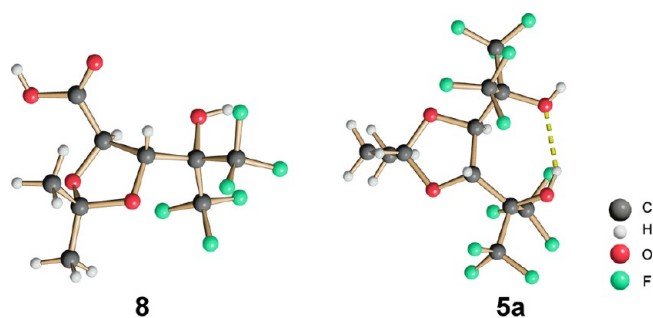


Figure 4. X-ray crystal structures of the tartaric acid bis-(trifluoromethyl) derivative 8 and of the tetrakis(trifluoromethyl) TEFDDOL 5a.

tube, and through a layer of 4 Å molecular sieves (see section 2.2.3 for the structure of the 2/1 complex of **5a** with water).

The crystal packing of the bis(trifluoromethyl) carboxylic acid **8** revealed numerous hydrogen-bonding interactions (Figure 5), which result in the aggregation of three molecules

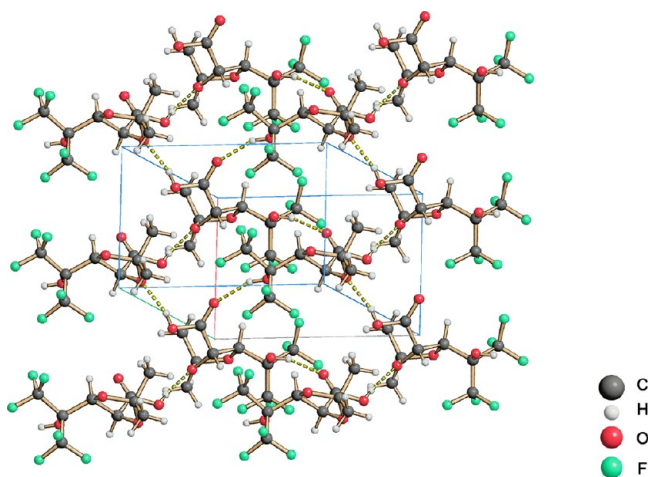


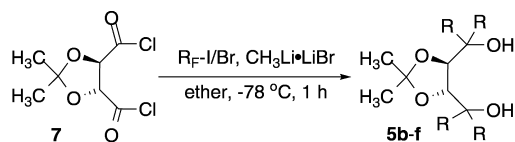
Figure 5. Crystal-packing diagram of the bis(trifluoromethyl) carboxylic acid **8**.

of **8** to form repeating “triplets”. The most prominent interaction is a hydrogen bond between the OH group of the carboxylic acid and one oxygen atom of the dioxolane ring of a neighboring molecule. A third molecule of **8** is involved, in the sense that the hydroxyl group of its fluoro alcohol moiety is hydrogen-bonded to the carbonyl oxygen atom of the first molecule (Figure 5).

As expected, the preparation of the tetrakis- CF_3 TEFDDOL **5a** was not successful when halogen–lithium exchange on CF_3I was tried for the generation of the CF_3 nucleophile. No trifluoromethylation of isopropylidene tartaric acid dichloride (**7**) could be observed. The latter result is not surprising, as it is well known that, even at low temperatures, (trifluoromethyl) lithium and the corresponding Grignard reagent are unstable and decompose instantaneously to difluorocarbene by elimination of the metal fluoride.¹³

2.1.2. Synthesis of the TEFDDOLs 5b–f Using Perfluorinated Organolithium Reagents. In our optimized procedure, isopropylidene tartaric acid dichloride (**7**) and the perfluorinated alkyl/aryl iodide or bromide (ca. 7 equiv) were dissolved together in diethyl ether at -78°C . Methyl lithium (5 equiv), complex with lithium bromide, was then added in one portion. After 1 h, aqueous workup followed by chromatographic purification afforded the desired products with yields ranging from 15 to 70% (Scheme 2).

Scheme 2. Synthesis of the TEFDDOLs **5b–f** Starting from Isopropylidene Tartaric Acid Dichloride (**7**)



5b: $\text{R} = \text{C}_2\text{F}_5$, 55 %; **5c:** $\text{R} = n\text{-C}_3\text{F}_7$, 25 %; **5d:** $\text{R} = n\text{-C}_4\text{F}_9$, 26 %;
5e: $\text{R} = n\text{-C}_6\text{F}_{13}$, 15 %; **5f:** $\text{R} = \text{C}_6\text{F}_5$, 70 %

Halogen–lithium exchange is sufficiently fast to be performed in the presence of the electrophile **7**—no side reactions of methyl lithium with tartaric acid dichloride **7** have been observed. With regard to the yields of TEFDDOLs **5b–f**, the in situ quenching method described above proved superior to the sequential formation of the (perfluoroalkyl)lithium intermediates, followed by addition of the acid chloride **7**. By the same token, the acid chloride **7** proved superior to other tartaric acid derived electrophiles, such as esters. As summarized in Scheme 2, we successfully introduced pentafluorophenyl, pentafluoroethyl, heptafluoro-*n*-propyl, nonafluoro-*n*-butyl, and tridecafluoro-*n*-hexyl groups using lithium–halogen exchange. As expected, CF_3I did not afford any of the CF_3 TEFDDOL **5a** under the conditions described above. However, as mentioned above (section 2.1.1), this “parent” TEFDDOL was accessible using Ruppert’s reagent ($\text{CF}_3\text{-TMS}$, **6**) as the trifluoromethyl source.

2.2. Solid-State Structures. **2.2.1. X-ray Crystal Structures of the TEFDDOLs 5a–f: Intramolecular Hydrogen Bonding in 5a–e, but not in 5f.** All TEFDDOLs **5a–f** were characterized by X-ray crystallography. The molecular structures of **5b–f** are shown in Figure 6. Note that all perfluoroalkyl TEFDDOLs **5b–e** show—just as the parent system **5a** (Figure 4)—the expected intramolecular OH–OH hydrogen bonding. In line with this, the pseudo-torsion angle $\text{O}-\text{C}_{\text{carbinol}}-\text{C}_{\text{carbinol}}-\text{O}$ is low and in the range of ca. $20\text{--}30^\circ$. As the sole exception, the tetrakis(pentafluorophenyl) TEFDDOL **5f** adopts a completely different conformation in the crystal: there is no intramolecular (and no intermolecular) OH–OH bonding. Instead, each of the two hydroxyl groups forms a bifurcated hydrogen bond to two “ortho” fluorine atoms on the phenyl rings. A pseudo-anti arrangement of the two hydroxyl groups results, with a pseudo-torsion angle $\text{O}-\text{C}_{\text{carbinol}}-\text{C}_{\text{carbinol}}-\text{O}$ of $170.7(2)^\circ$. The H–F distances are in the range 2.23–2.29 Å. These values coincide very well with the H–F bond length of 2.23 Å observed earlier in intramolecularly H–F bonded 2-fluorophenyldiphenylmethanol.¹⁹

Note that in the area of TADDOLs, of the 161 crystal structures deposited in the CCDC file, only two show the pseudo-anti arrangement of the two hydroxyl groups.²⁰ In both of these cases, the TADDOL incorporates a diphenyldioxolane (i.e., a benzophenone acetal). Thus, **5f** is the only case of a dimethyldioxolane (i.e., acetone acetal) showing a pseudo-anti conformation. In the case of the two TADDOLs, the pseudo-anti conformation is enforced by nonbonding interactions involving the acetalic phenyl groups. In other words, steric hindrance overrides the attractive intramolecular OH–OH bonding. In the case of the tetrakis(pentafluorophenyl) TEFDDOL **5f**, a total of four intramolecular OH–F bonds override one OH–OH bond. Note that the pseudo-anti conformation of TEFDDOL **5f** persists in solution (see section 2.3); thus, it is clearly not an effect of crystal packing.

2.2.2. X-ray Crystal Structures of the TEFDDOLs 5a–f: Modes of Intermolecular Hydrogen Bonding. To our delight, the X-ray crystal structure of the tetrakis(trifluoromethyl) TEFDDOL **5a** (Figure 7), which could be obtained in water-free form by sublimation through molecular sieves (4 Å), revealed a hydrogen-bond network reminiscent of that found for HFIP (**4**) itself.¹⁰ Most importantly, the OH groups of **5a** form an endless, zigzag-patterned ribbon. In this endless sequence of intra- and intermolecular hydrogen bonds, the intramolecular O–H–O bonds have an O–O distance of 2.752 Å (average over the three independent molecules in the unit

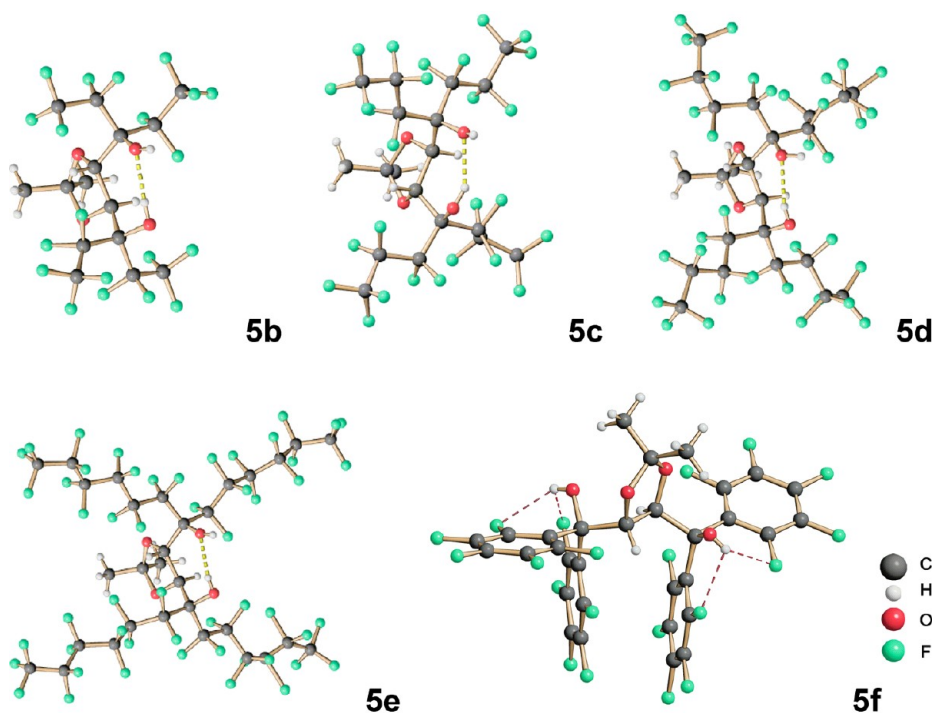


Figure 6. Crystal structures of TEFDDOLs **5b–f**. Disorder of OH H atoms is not shown. The C_2F_5 groups of **5b** are disordered, and only one orientation is shown.

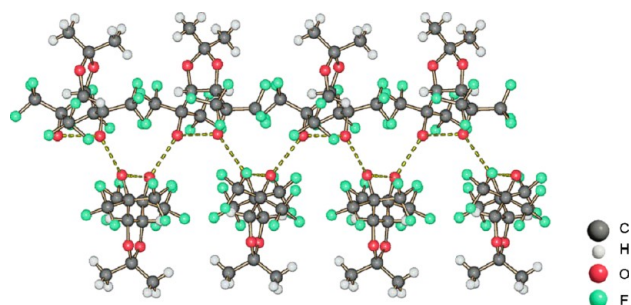


Figure 7. Layered crystal packing of intra- and intermolecular hydrogen-bonded TEFDDOL **5a**.

cell), whereas the intermolecular bonds are on the average 3.079 Å in length. Furthermore, it is interesting to note that the crystal shows a trifle-type separation of the polar OH regime, mantled by fluorous layers which are made up by the closely interacting CF_3 groups. These fluorous layers are again followed by a medium-polarity “hydrocarbon” layer, consisting of the dioxolane’s oxygen atoms and the methyl groups of **5a**’s acetal substructure (Figure 7).

The crystal structures of tetrakis(pentafluoroethyl) TEFDDOL **5b** and its homologue **5c** revealed a different mode of intermolecular hydrogen-bonding interaction. As shown in Figure 8, these TEFDDOLs are characterized by hydrogen-bonded dimers. Dimerization is brought about by intermolecular hydrogen O–H–O bonding, typically 2.745 Å in length, in addition to the typical intramolecular O–H–O bonding

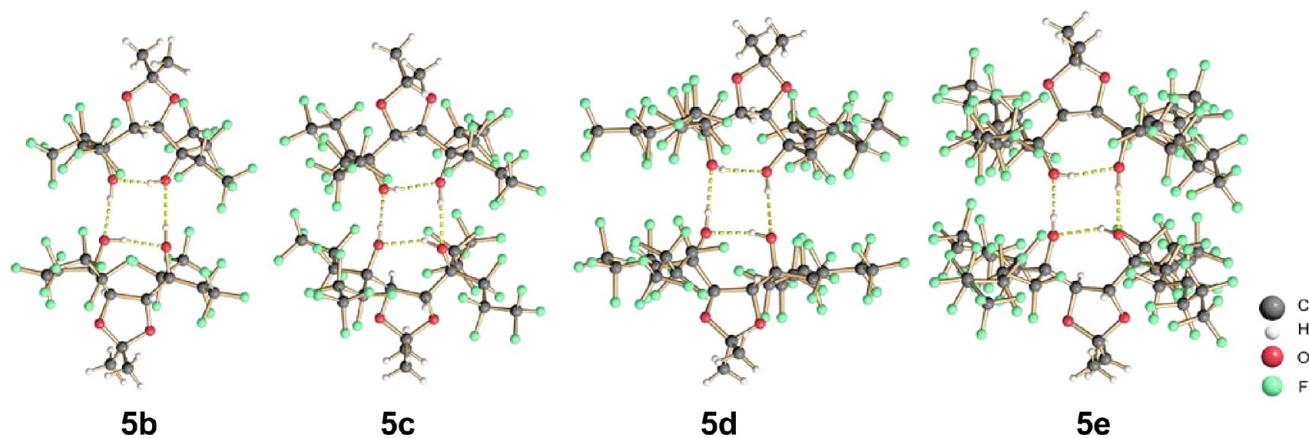


Figure 8. Cyclic hydrogen-bond networks observed for the tetrakis(pentafluoroethyl) (**5b**), the tetrakis(heptafluoro-*n*-propyl) (**5c**), the tetrakis(nonafluoro-*n*-butyl) (**5d**), and the tetrakis(tridecafluoro-*n*-hexyl) TEFDDOLs (**5e**). Disorder of OH H atoms is not shown. The C_2F_5 groups of **5b** are disordered, and only one orientation is shown.

(2.695 Å on the average). Most likely, the increasing size of the perfluoroalkyl groups (C_2F_5 , and C_3F_7 vs CF_3) prohibits the formation of endless H-bonded aggregates (as in **5a**, Figure 7), and accounts for the observed change in packing. The higher TEFDDOL homologues **5d,e** form dimers with an analogous hydrogen-bonding pattern (Figure 8). Note that, in the area of fluorinated monoalcohols, similar oligomers, with analogous eight-membered cyclic hydrogen bond networks, are observed e.g. for racemic 1-phenyl-2,2,2-trifluoroethanol.^{10,29}

The crystal structure of the tetrakis(pentafluorophenyl) TEFDDOL **5f** revealed a completely different aggregation mode of the individual molecules. Unlike all other TEFDDOLs, and almost all TADDOLs which have an intramolecular O–H–O hydrogen bond, this is not the case for the TEFDDOL **5f**. Instead, its hydroxyl groups are involved in both intra- and intermolecular O–H–F bonding (Figure 9).

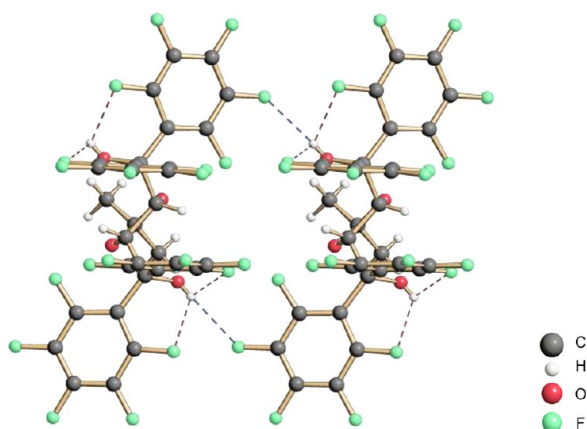


Figure 9. Intra- and intermolecular OH–F hydrogen bonding in tetrakis(pentafluorophenyl) TEFDDOL **5f**.

As mentioned before, each one of TEFDDOL **5f**'s hydroxyl groups forms a bifurcated hydrogen bond to two ortho fluorine atoms on the phenyl rings (Figure 9, marked in red). In the crystal, a third—now intermolecular—interaction exists between the hydroxyl groups' H atom and a meta fluorine atom of a neighboring TEFDDOL molecule (Figure 9, marked in blue). For the intermolecular OH–F bonds, the H–F distances were found to be in the range of 2.33–2.46 Å—significantly below the sum of the van der Waals radii of the two atoms (267 pm). Clearly, also the lengths of the intramolecular OH–F bonds in TEFDDOL **5f** (2.23–2.29 Å, see above) fall significantly below this value.

An earlier analysis of hydrogen bonding involving organic fluorine as acceptor (in 1997 by Dunitz and Taylor, based mainly on crystal structures) came to the conclusion that this type of interaction occurs only scarcely.²¹ A very recent (2012) discussion of the topic by Schneider, including spectroscopy, association equilibria in solution, and computational studies, points to a much more widespread occurrence and importance of hydrogen bonding to fluorine.²² We feel that TEFDDOL **5f** is a good example of the importance of OH–F bonding, with regard to both molecular conformation and aggregation.

2.2.3. X-ray Crystal Structures of the TEFDDOLs 5a–f in the Presence of Lewis Bases: Complexes with Hydrogen Bond Acceptors. Water as the Second Component. We also obtained crystallographic data of TEFDDOL **5a** as a 2/1 complex with water (Figure 10). In this hydrate, again an

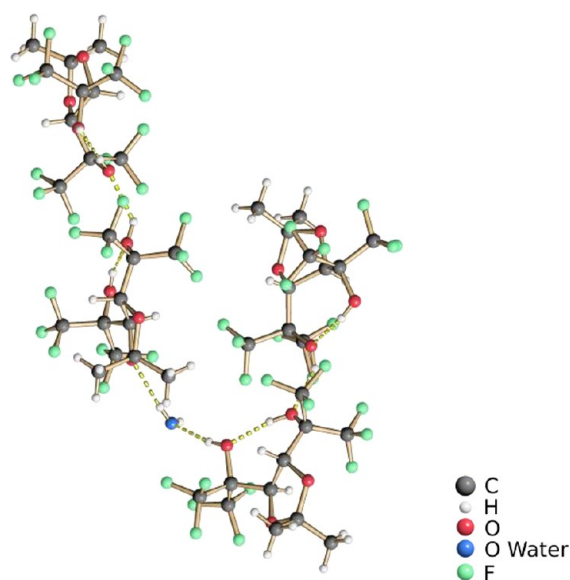


Figure 10. 2/1 complex of TEFDDOL **5a** with H_2O .

intramolecular hydrogen bond between the two hydroxyl groups of each TEFDDOL monomer is visible. Two TEFDDOL monomers dimerize, similar to the aggregation mode seen in water-free TEFDDOL **5a** (Figure 7). The terminal activated hydroxyl group of the dimer then forms an intermolecular hydrogen bond to water, which itself donates another intermolecular hydrogen bond to one of the oxygen atoms of the dioxolane ring of a TEFDDOL from the next TEFDDOL dimer. Overall, an endless hydrogen-bonded $[5a_2 \cdot H_2O]_n$ aggregate results (Figure 10). The crystal structure of the 2/1 complex of the tetrakis(pentafluoroethyl) TEFDDOL **5b** with water revealed a rather similar hydrogen-bonding pattern, giving rise to an endless $[5b_2 \cdot H_2O]_n$ aggregate (Figure 11).

Amines (DABCO and Piperidine) As the Second Component. In the cases of the pentafluoroethyl TEFDDOL **5b** and the pentafluorophenyl TEFDDOL **5f**, we have also prepared

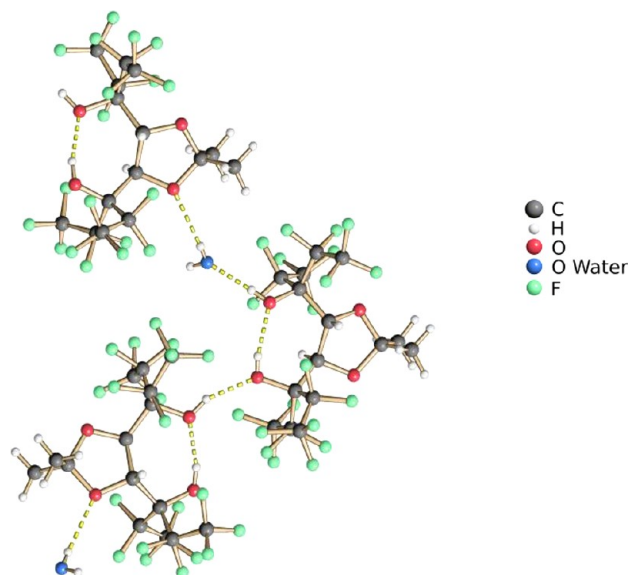


Figure 11. 2/1 complex of TEFDDOL **5b** with H_2O .

and characterized complexes with amine bases, in particular with piperidine and DABCO (1,4-diazabicyclo[2.2.2]octane).

The crystal structure of the complex of **5b** with DABCO is shown in Figure 12. The composition of this material can be

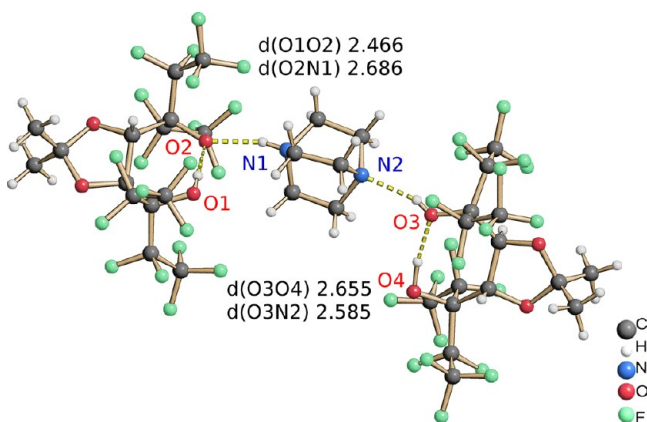


Figure 12. 2:1 complex of TEFDDOL **5b** with DABCO.

described as a [TEFDDOL-H⁺·DABCO+H⁺·TEFDDOL] salt. As should be the case, the tertiary diamine ($pK_a(\text{DMSO}) = 8.93, 2.97$)²³ is monoprotonated by one of two tetrakis-(pentafluoroethyl) TEFDDOL (**5b**) molecules. Once again, intramolecular H bonds exist between the hydroxyl groups of the two TEFDDOL units ($d_{\text{O1O2}} = 2.466(6)$ Å, $d_{\text{O3O4}} = 2.655(8)$ Å). It is evident from these bond lengths that one of the two TEFDDOL molecules is deprotonated: i.e., has transferred the exocyclic proton to the amine. In Figure 12, the deprotonated TEFDDOL unit is the one to the left, harboring O1 and O2. The TEFDDOL molecule to the right appears to just form a strong hydrogen bond to the second N atom of DABCO. Overall, two intermolecular hydrogen bonds exist between the N atoms of DABCO and the activated hydroxyl groups of the two TEFDDOL molecules ($d_{\text{N1O2}} = 2.686(6)$ Å, $d_{\text{N2O3}} = 2.585(7)$ Å).

With DABCO as the proton acceptor, also the less acidic tetrakis(pentafluorophenyl) TEFDDOL **5f** forms a salt (Figure 13). In the 2/3 complex of C₆F₅ TEFDDOL **5f** with DABCO, we see two independent H-bridged ion pairs of DABCO +H⁺·**5f**-H⁺ (left and right in Figure 13). The relatively short O–O distances within the TEFDDOL moieties are indicative of the deprotonated state ($d_{\text{O1O2}} = 2.561(3)$ Å, $d_{\text{O3O4}} = 2.620(4)$ Å). It is interesting to note that in the deprotonated state, the TEFDDOL **5f** adopts the conformation typical for all

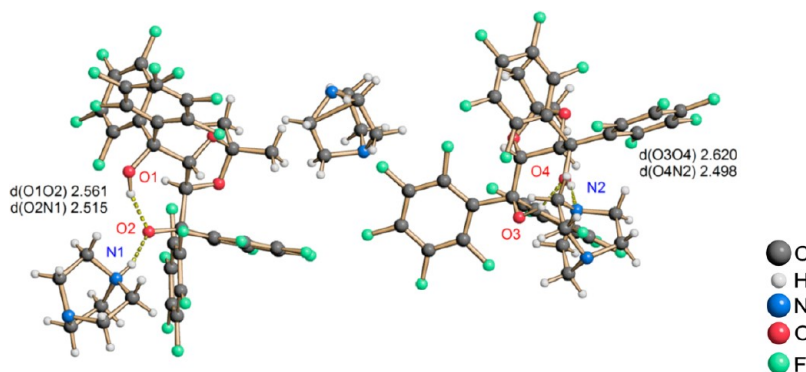


Figure 13. 2/3 complex of TEFDDOL **5f** with DABCO.

other TEFDDOLs: i.e., showing an intramolecular OH–O hydrogen bond. In other words, single OH hydrogen bonding to the anionic carbinolate oxygen atom overrides two bifurcated OH–F hydrogen bonds. A third DABCO molecule occupies a central position as a non-hydrogen-bonded guest molecule.

Not surprisingly, in the complex of the tetrakis-(pentafluorophenyl) TEFDDOL **5f** with the more basic piperidine ($pK_a(\text{DMSO}) = 10.85$)²⁴, the TEFDDOL is deprotonated as well (Figure 14). In this 1/2 complex, a cyclic

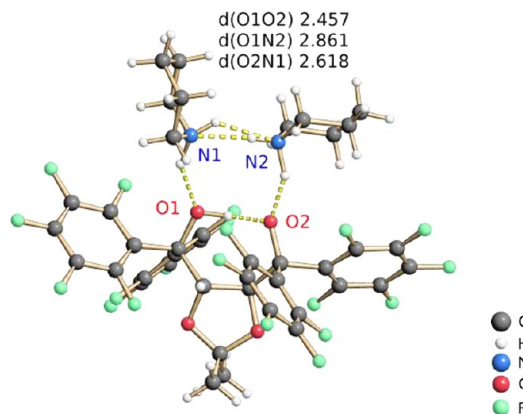


Figure 14. 1:2 complex of the tetrakis(pentafluorophenyl) TEFDDOL **5f** with piperidine (hydrogen atoms in the N–H–N bridge are disordered).

hydrogen-bond network is completed by incorporation of a second piperidine molecule. In this arrangement, the TEFDDOL OH–O distance is short ($d_{\text{O1O2}} = 2.457(3)$ Å), indicative of deprotonation of the TEFDDOL moiety.

2.3. TEFDDOL Structures in Solution. The conformational and aggregational behavior of the tetrakis-C₂F₅ TEFDDOL **5b** and of the tetrakis-C₆F₅ TEFDDOL **5f** (Figure 15) in solution was investigated by NOE and by DOSY NMR spectroscopy, respectively (¹H, ¹⁹F).

2.3.1. TEFDDOL Conformations in Solution: NOE Experiments. For the tetrakis-C₂F₅ TEFDDOL **5b**, the pseudo-syn orientation of the intramolecularly hydrogen bonded hydroxyl functions (see Figures 6 and 8) could be also confirmed for the solution structure of **5b** (Figure 16). In the homonuclear F,F NOESY spectrum, the two nonequivalent pentafluoroethyl groups can be assigned, while the H,F HOESY experiment served to distinguish between the two putative conformers for the signal set observed. In particular, the very strong cross

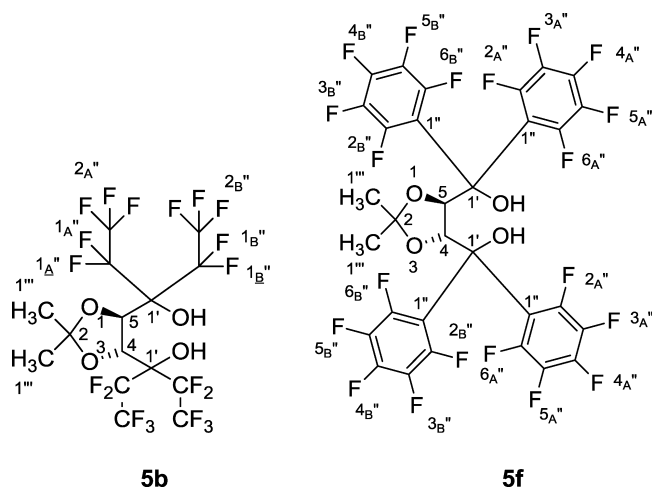


Figure 15. Numbering scheme for TEFDOLs **5b,f** investigated by NMR spectroscopy.

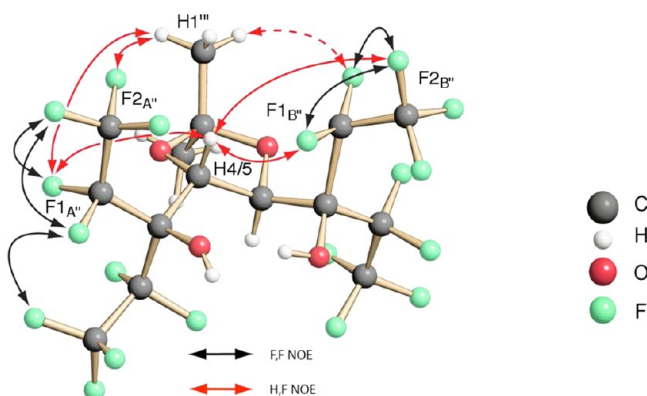


Figure 16. NOEs observed for the TEFDOL **5b**. For reasons of clarity, the second **5b** molecule present in the dimeric aggregate is not shown. See the Supporting Information for the original NOESY spectra.

peaks between H4/5 and F2_{B''}—or H4/5 and F1_{B''}—(see Figure 15 for atom numbering) are not expected for a conformation where the two OH functionalities are pointing in opposite directions from the plane of the five-membered ring (pseudo-anti). In contrast, no cross peak is observed between H4/5 and F1_{A''} and only a very weak NOE between H4/5 and F1_{A''}, which cannot be accounted for by a pseudo-anti conformer. Likewise, the nonexistence of a cross peak for H1^{'''} and F2_{B''} together with the strong NOE for H1^{'''} and F2_{A''} can only be explained by a pseudo-syn arrangement of the hydroxyl groups with respect to each other.

For the tetrakis-C₆F₅ TEFDOL **5f**—as also indicated by diffusion measurements (see below)—a monomeric structure is supported by NOE data as well. Homo- and heteronuclear NOE experiments were performed. In particular, the two-dimensional H₁F HOESY spectra show that in solution, as in the solid state (compare Figure 6), a pseudo-anti arrangement of the two OH groups is preferred (Figure 17). In other words, also in CDCl₃ solution, the molecule's conformation is dominated by intramolecular OH–F bonding. Distance evaluation for possible pseudo-syn and pseudo-anti conformers, with the first one forming a possible dimer, and comparison with NOE data led to the assignment given in section 4. A very strong NOE between H4/5 and F2_{B''}/F6_{B''}, which is attributed

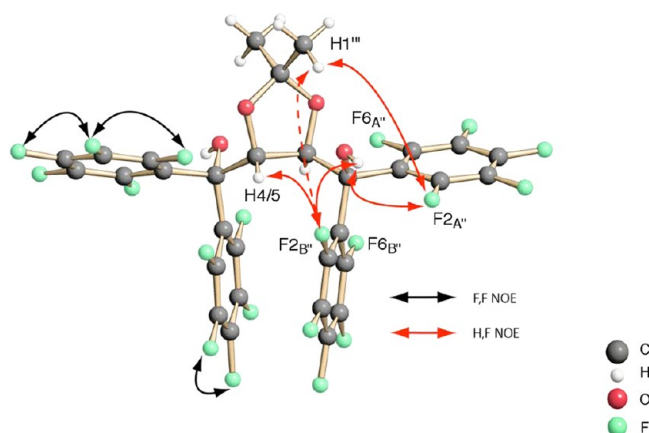


Figure 17. NOEs observed for the TEFDOL **5f**. See the Supporting Information for the original NOESY spectra.

to the NOE between each of the two identical stacked C₆F₅ unit's interaction with the methine group, and also the strong NOEs between the hydroxyl protons and F2_{A''}/F6_{A''} and F2_{B''}/F6_{B''}, as well as H1^{'''} and F2_{A''}/F6_{A''} are in favor of this interpretation. At the same time, missing NOE contacts between H1^{'''} and F4_{B''} or F3_{B''}/F5_{B''}, respectively, clearly would be in contradiction with a pseudo-syn form and therefore further support our conclusions.

2.3.2. Supramolecular Structures in Solution: DOSY Experiments. For the tetrakis(pentafluoroethyl) TEFDOL **5b**, diffusion measurements were recorded for a series of different concentrations, ranging from 0.8 to 12.5 mM (in CDCl₃). As can be seen from the plot of diffusion coefficients vs concentration (Figure 18), at diol concentrations below 0.01

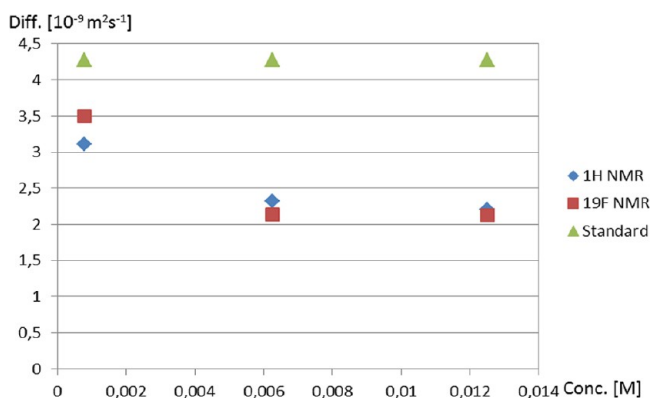


Figure 18. TEFDOL **5b**: diffusion coefficient in CDCl₃ as a function of concentration. TMS was used as the standard. See the Supporting Information.

M, an increase in diffusion coefficient—which is equivalent to a larger fraction of monomeric species—can be observed. As has been suggested earlier, changes in hydrodynamic radii upon formation or breaking of H bonds can be gauged by using TMS as an internal diffusion reference.²⁵ By comparison of experimentally determined diffusion coefficients and the relative change in hydrodynamic radius, a value of D/D^{TMS} of ca. 0.5 for the concentrations of 12.5 mM and above vs D/D^{TMS} of 0.73 for the most dilute solution under investigation and a corresponding change of the hydrodynamic radius, Δr_{H} , by ca. 1.4 were obtained. This result can be interpreted by the TEFDOL **5b** existing in an aggregation state close to

monomeric in solutions of concentration ca. 0.8 mM or below. Note that this value was determined in chloroform as solvent, which has very low hydrogen bond accepting capacity. We interpret the aggregation state being populated at higher concentrations as the H-bonded dimer found in the crystal structure of TEFDDOL **5b** (Figure 8).

A similar set of diffusion experiments was carried out for the tetrakis(pentafluorophenyl) TEFDDOL **5f**. In contrast to the changes observed for increasingly dilute solutions of the TEFDDOL **5b**, when diffusion experiments were recorded with **5f**, almost no changes in diffusion coefficient were visible throughout the investigated range of concentrations (Figure 19). At the same time, the absolute values of diffusion

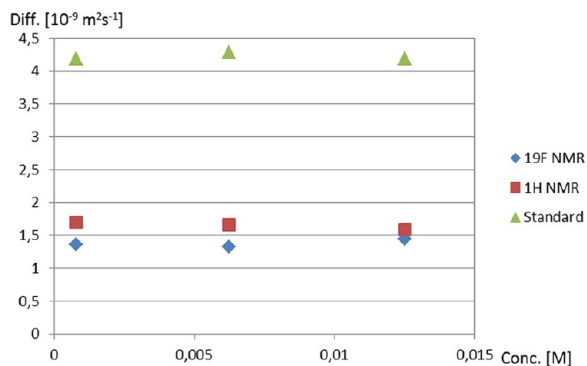


Figure 19. TEFDDOL **5f**: diffusion coefficient in CDCl_3 as a function of concentration. TMS was used as the standard. See the Supporting Information.

coefficients match those expected for the monomeric TEFDDOL **5f** in chloroform solution. In other words, the tetrakis(pentafluorophenyl) TEFDDOL **5f** does not show any tendency toward aggregation in chloroform solution up to at least 12.5 mM concentration. This result indicates that the third and intermolecular OH–F hydrogen bond found in the crystal structure of **5f** (Figure 9, H bonds indicated in blue) is weak and does not persist in solution.

2.4. Miscellaneous. **2.4.1. Attempted Synthesis of the meso-TEFDDOL 9.** Under the same reaction conditions as described above (section 2.1.2), we have tried to synthesize an achiral counterpart of the tetrakis(pentafluoroethyl) TEFDDOL **2b**: namely, the *meso*-TEFDDOL **9** (Figure 20). For the

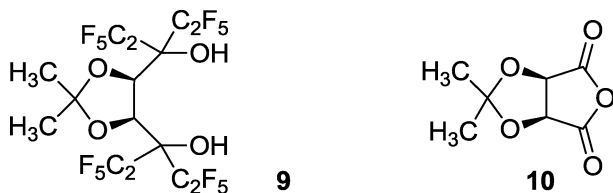


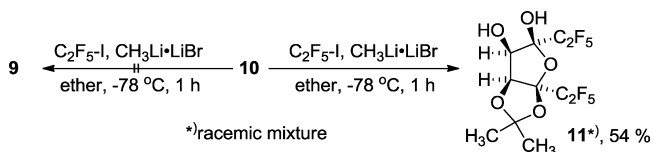
Figure 20. Formulas of the desired *meso*-TEFDDOL **9** and of isopropylidene *meso*-tartaric anhydride **10**.

preparation of the required *meso*-tartaric dichloride, we applied the procedure by Klotz et al. for the synthesis of the chiral tartaric dichloride **7**.¹⁷ However, treatment of the *meso*-tartaric disodium salt with thionyl chloride furnished the anhydride **10**, which was employed for further experimentation.

As described in section 2.1.2, pentafluoroethyl iodide and the anhydride **10** were dissolved in diethyl ether at -78°C and methyllithium, complex with lithium bromide, was added.

Under these conditions, no indication for the formation of the desired *meso*-TEFDDOL **9** was obtained. Instead, the product *rac*-**11** with only two pentafluoroethyl groups was isolated (Scheme 3).

Scheme 3. Synthesis of *rac*-**11** Starting from the Isopropylidene Protected Anhydride **10**



The X-ray crystal structure of *rac*-**11** is shown in Figure 21. In the crystal, the enantiomers of *rac*-**11** form heterochiral

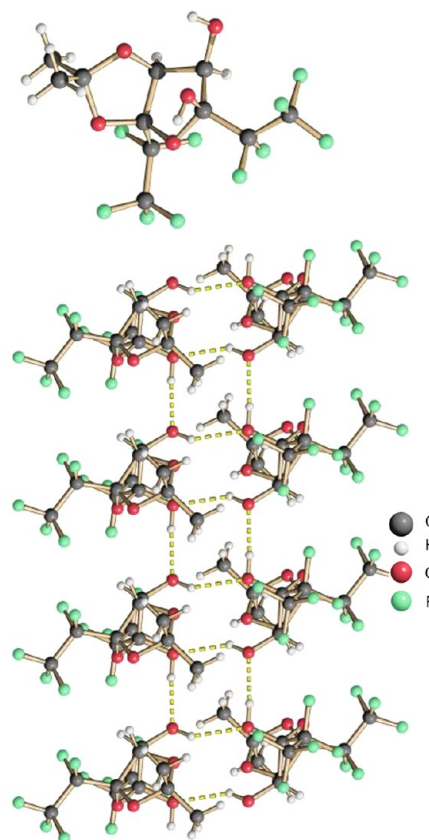
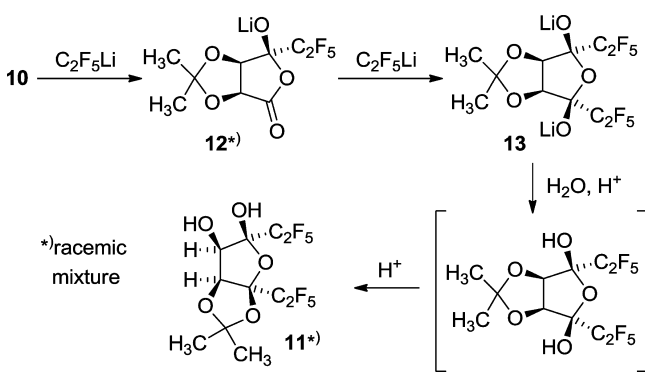


Figure 21. X-ray crystal structure of compound *rac*-**11**: (top) molecular structure; (bottom) intermolecular hydrogen bonding pattern.

hydrogen-bonded dimers (horizontal hydrogen bonds in Figure 21). The latter dimers aggregate, again by hydrogen bonding (vertical H bonds in Figure 21), to endless ribbons.

The formation of the unexpected product *rac*-**11** from the *meso*-tartaric anhydride **10** can be explained as summarized in Scheme 4. Initial *exo* attack of (pentafluoroethyl)lithium on the bicyclic anhydride **10** affords the alcoholate *rac*-**12**. A second *exo* attack on the remaining carbonyl group furnishes the diolate *meso*-**13**. As the final step, transacetalization—most likely during acidic workup—affords *rac*-**11**. The latter process is facilitated by the *cis* orientation of the hydroxyl groups involved.

Scheme 4. Suggested Mechanism for the Formation of the Diol *rac*-11

2.4.2. pK_a Values of the TEFDDOLs **5a,b,f.** We recently disclosed the pK_a values of the TEFDDOLs **5a,b,f** in DMSO.¹¹ It was found that the tetrakis(perfluoroalkyl) TEFDDOLs **5a,b** are rather acidic (pK_a (**5a**) = 5.7; pK_a (**5b**) = 2.4), whereas the tetrakis(pentafluorophenyl) TEFDDOL **5f** has a pK_a value of ca. 11. Clearly, intramolecular hydrogen bonding accounts for the increased acidity of the tetrakis(perfluoroalkanedioles) **5a,b** relative to the monomeric 1,1,1,3,3,3-hexafluoro-2-propanol (HFIP, pK_a = 17.2¹¹). In the case of the tetrakis(pentafluorophenyl) TEFDDOL **5f**, the pK_a of ca. 11 is basically identical with that of the monomeric decafluorobenzhydrol (ca. 11).¹¹ In other words, the hydroxyl groups of **5f** act independently—consistent with TEFDDOL **5f**'s preferred pseudo-anti conformation, both in the crystal (Figures 6 and 9) and in solution (Figure 17).

3. CONCLUSIONS

(i) We have established a versatile one-step synthesis for a novel class of chiral and highly fluorinated diols, the TEFDDOLs ($\alpha,\alpha,\alpha',\alpha'$ -tetrakis(perfluoroaryl/alkyl)-5,5'-dimethyl-1,3-dioxolane-4,5-dimethanols).

(ii) All perfluoroalkyl TEFDDOLs (**5a–e**) show intramolecular HO–HO hydrogen bonding, both in the solid state and in solution (pseudo-syn orientation of the H-bonded OH groups). As a result, the perfluoroalkyl TEFDDOLs show acidity significantly higher than that of the parent fluorinated monoalcohols. pK_a values as low as 2.4 were measured, which make the TEFDDOLs promising candidates for applications in asymmetric organocatalysis.

(iii) In the tetrakis(pentafluorophenyl) TEFDDOL **5f**, the overall conformation is dictated by bifurcated intramolecular hydrogen bonding between the molecule's OH groups and the ortho fluorine atoms of the C_6F_5 rings. This interaction overrides the molecule's intrinsic potential for intramolecular HO–HO hydrogen bonding, and a pseudo-anti arrangement of the OH groups results. As a consequence of the non-cooperativity of its OH groups, the tetrakis(pentafluorophenyl) TEFDDOL **5f** does not show enhanced acidity relative to its monoalcohol decafluorobenzhydrol.

(iv) In the solid state, the pure perfluoroalkyl TEFDDOLs **5a–e** form aggregates (dimers or infinite ribbons) by intermolecular hydrogen bonding. Furthermore, these aggregates are characterized by a strict layering of the perfluoroalkyl groups, the highly polar OH groups, and the dioxolane residues of medium polarity.

(v) An analogous layering is observed for the tetrakis(pentafluorophenyl) TEFDDOL **5f**. Intermolecular bonding,

however, is effected by weak OH–F interactions and not by HO–HO bonds.

(vi) In chloroform solution, the conformational features found in the crystal for both the perfluoroalkyl and perfluorophenyl TEFDDOLs **5b,f** persist. The monomeric tetrakis(perfluoroethyl) TEFDDOL **5b** is in equilibrium with a dimer, which prevails at higher concentrations. In contrast, the tetrakis(perfluorophenyl) TEFDDOL **5f** shows no tendency toward aggregation.

(vii) In the presence of Lewis bases (water, amines), all TEFDDOLs form well-defined aggregates in the solid state. The TEFDDOL's diol substructure acts as a monodentate hydrogen-bond donor.

(viii) In the presence of sufficiently Brønsted basic partners (amines), the TEFDDOLs may become deprotonated and can form crystalline ammonium salts. For the tetrakis(pentafluorophenyl) TEFDDOL **5f**, deprotonation is accompanied by a dramatic change in conformation (in the crystal): in its anion, OH–F hydrogen bonding is overridden, and a conformation with an intramolecular OH–O hydrogen bond results (i.e., the conformation typical for all tetrakis(perfluoroalkyl) TEFDDOLs).

Future studies in our laboratory will be devoted to potential applications of this new class of chiral fluorodiols, in particular with regard to their potential as chiral Brønsted acids or building blocks for chiral ligands.

4. EXPERIMENTAL SECTION

4.1. General Information. All reactions were carried out under an argon atmosphere and in flame-dried glassware, using standard Schlenk techniques. Reagents were purchased from standard suppliers and were used without further purification. Solvents were dried according to general procedures.²⁶ TLC spots were visualized by fluorescent indicator or by cerium–molybdenum spray reagent. Flash chromatography was performed on silica gel. Gas chromatography (GC): helium used as a carrier gas, HP-5 MS or Optima 5 Accent (Macherey-Nagel) 30 m \times 0.25 mm capillary columns. GC data are given as follows: type of the column, GC method in the following formula: initial temperature (min) \rightarrow ramp ($^{\circ}\text{C}/\text{min}$) \rightarrow final temperature (min).

For nuclear magnetic resonance (NMR), ^1H and ^{13}C chemical shifts (δ) are given in ppm relative to the solvent reference as an internal standard. Assignments are supported by H,H COSY, H,C HMQC, and H,C HMBC spectra. Gradient-selected F,F COSY, F,C HMBC, and H,F HOESY²⁷ spectra were recorded using an inverse H,F TBI probe, equipped with a pulsed gradient unit capable of producing magnetic field pulse gradients in the z direction of 56 G cm^{-1} . Data are reported as follows: chemical shift (multiplicity (s for singlet, d for doublet, t for triplet, q for quartet, sept for septet, m for multiplet), coupling constant (Hz), integration, assignment). For the attribution of scalar couplings, ^{19}F NMR spectra were simulated with SpinWorks 3.1.7 (K. Marat, University of Manitoba, 2010) using NUMRIT algorithms.²⁸ For the numbering scheme of ^{19}F NMR assignments, see Figure 15.

High-resolution mass spectra (HR-MS) were recorded in ESI mode, using a quadrupole ion trap (EB-Q-trap).

For Fourier transform infrared spectroscopy (FT-IR), absorption bands are given in wavenumbers ($\tilde{\nu}$, cm^{-1}). Intensities of the bands are given as follows: s for strong peaks, m for peaks with medium intensity, and w for weak bands. Broad absorptions are denoted by br.

Melting points (mp) are uncorrected.

For X-ray crystal structure analysis, structures were solved using SHELXS97 and refined with SHELXL97.

For optical rotations, concentrations c are given in g/100 mL.

4.2. Preparation of the Acid Chloride **7 and Anhydride **10**.**
4.2.1. (4*R*,5*R*)-2,2-Dimethyl-1,3-dioxolan-4,5-dicarbonyl Dichloride (7**).** This acid chloride was prepared according to Klotz et al.¹⁷ Yield (from 1.00 g of the disodium salt): 780 mg (3.45 mmol, 81%; lit. yield

69%). Colorless crystals were obtained by sublimation (10^{-2} mbar, 50 °C); mp 40–42 °C. ^1H NMR (300.1 MHz, CDCl_3): δ 5.20 (s; 2H), 1.56 (s; 6H). ^{13}C NMR (75.5 MHz, CDCl_3): δ 172.1, 117.4, 83.7, 26.8. ESI-MS (pos): m/z (%) 227 (11) [M^+]. IR: $\tilde{\nu}$ 2993 (w), 2945 (w), 1776 (s), 1455 (w), 1377 (m), 1230 (m), 1122 (m), 1008 (m), 982 (w), 954 (w), 825 (w), 746 (w), 695 (w), 652 (w), 599 (w) cm^{-1} .

X-ray structural data of **7** (CCDC 827655): $\text{C}_7\text{H}_8\text{Cl}_2\text{O}_4$, formula weight 227.03, crystal size $0.30 \times 0.20 \times 0.10$ mm, crystal system monoclinic, space group C2, unit cell dimensions $a = 14.2526(12)$ Å, $b = 8.9791(10)$ Å, $c = 9.7106(5)$ Å, $\beta = 129.481(4)^\circ$, $Z = 4$, $D_{\text{calcd}} 1.572$ g cm^{-3} , absorption coefficient 0.655 mm^{-1} , wavelength 0.71073 Å, $T = 100(2)$ K, $2\theta_{\text{max}} = 27.00^\circ$, 35 033/9028 collected/unique reflections ($R(\text{int}) = 0.0202$), final R indices ($I > 2\sigma(I)$) $R = 0.0301$, $R_w = 0.0652$, largest diff peak and hole 0.219 and -0.290 $\text{e} \text{Å}^{-3}$.

4.2.2. (3aR,6aS)-2,2-Dimethylfuro[3,4-d][1,3]dioxole-4,6-(3aH,6aH)-dione (10). This acid anhydride was prepared analogously to the procedure by Klotz et al.¹⁷ Yield (from 1.50 g of the disodium salt): 510 mg (1.97 mmol, 46%). Colorless crystals were obtained by sublimation (10^{-2} mbar, 60 °C); mp 49–51 °C. ^1H NMR (300.1 MHz, CDCl_3): δ 5.16 (s; 2H), 1.51 (s; 6H). ^{13}C NMR (75.5 MHz, CDCl_3): δ 172.1, 117.4, 83.7, 26.9. GCMS: $\tau_R = 14.61$ min; m/z 207, 189, 176, 158, 145, 129, 115, 101, 85, 73, 59; Macherey Optima-5MS; 35 °C, 5 min, 20 °C/min \rightarrow 280 °C, 10 min. ESI-MS (pos): m/z (%) 195 [$\text{M}^+ + \text{Na}^+$] (16), 173 [$\text{M}^+ + \text{H}^+$] (100). IR: $\tilde{\nu}$ 3534 (w), 3312 (br), 2822 (br), 2623 (br), 2488 (br), 1713 (s), 1682 (s), 1439 (m), 1306 (m), 1252 (m), 1207 (s), 1125 (m), 1098 (s), 914 (m), 874 (m), 822, (m) 743 (m) cm^{-1} .

X-ray structural data of **10** (CCDC 827664): $\text{C}_7\text{H}_8\text{O}_5$, formula weight 172.13, crystal size $0.40 \times 0.40 \times 0.15$ mm, crystal system monoclinic, space group $P2_1/c$, unit cell dimensions $a = 8.7026(10)$ Å, $b = 7.6311(8)$ Å, $c = 11.557(2)$ Å, $\beta = 103.131(4)^\circ$, $Z = 4$, $D_{\text{calcd}} 1.530$ g cm^{-3} , absorption coefficient 0.133 mm^{-1} , wavelength 0.71073 Å, $T = 100(2)$ K, $2\theta_{\text{max}} = 27.00^\circ$, 3691/1630 collected/unique reflections ($R(\text{int}) = 0.0407$), final R indices ($I > 2\sigma(I)$) $R = 0.0349$, $R_w = 0.0762$, largest diff peak and hole 0.171 and -0.228 $\text{e} \text{Å}^{-3}$.

4.3. Preparation of the Tetrakis(trifluoromethyl)-TEFDDOL 5a and of the Carboxylic Acid 8 by using Ruppert's Reagent (6). **4.3.1. [(4R,5R)-2,2-Dimethyl-1,3-dioxolane-4,5-diy]bis-(1,1,1,3,3,3-hexafluoropropan-2-ol) (5a).** The tartaric acid dichloride **7** (1.00 g, 1.00 equiv, 4.30 mmol) was dissolved in 25 mL of glyme, and the solution was cooled to -50 °C. Trimethyl(trifluoromethyl)silane (**6**; 4.65 mL, 7.10 equiv, 31.42 mmol) and tetramethylammonium fluoride (TMAF, 2.93 g, 7.10 equiv, 31.42 mmol) were added at -50 °C. The reaction mixture was stirred for 1 h at -30 °C and then overnight at room temperature. Saturated aqueous NH_4Cl was added (30 mL). The layers were separated, and the aqueous phase was extracted with diethyl ether. The combined organic extracts were dried over MgSO_4 , and the solvent was evaporated in vacuo. The crude product (yellowish brown oil) was purified by flash chromatography (cyclohexane/EtOAc 1/1) and subsequent sublimation or crystallization to give the trifluoromethylated reaction product **5a** as colorless crystals.

Water-free colorless crystals (374 mg, 20%) were obtained by sublimation at 50 °C under vacuum (10^{-2} mbar) in a sealed tube and through a layer of 4 Å molecular sieves: mp 104–105 °C. $[\alpha]_D^{20} = +4.6^\circ$ (c 0.6, CHCl_3). ^1H NMR (300.1 MHz, CDCl_3): δ 4.78 (s; 2H), 1.48 (s; 6H), OH not detected. ^{13}C NMR (75.5 MHz, CDCl_3): δ 122.2, 121.5, 113.9, 78.1, 75.2, 26.6. ^{19}F NMR (282.4 MHz, CDCl_3): δ -71.45 (q; 6F, $F-1_A''$, $^4J_{\text{FF}} = 9.0$ Hz), 75.89 (q; 6F, $F-1_B''$, $^4J_{\text{FF}} = 9.0$ Hz). GCMS: $\tau_R = 8.55$ min; m/z 420, 419, 395, 267, 251, 238, 169, 147, 121, 97, 91, 85, 78, 69, 59, 55; Macherey Optima-5MS; 35 °C, 5 min, 20 °C/min \rightarrow 280 °C, 10 min. ESI-MS (neg): m/z (%) 433 [$\text{M} - \text{H}^+$] (99). IR: $\tilde{\nu}$ 3269 (br), 2999 (w), 2963 (w), 1674 (w), 1468 (w), 1379 (w), 1279 (w), 1244 (w), 1244 (s), 1204 (s), 1146 (s), 1128 (s), 1090 (s), 1065 (m), 1053 (m), 982 (m), 957 (m), 880 (m), 810 (m), 799 (m), 737 (m), 721 (m), 689 (w), 660 (w), 625 (w), 606 (w) cm^{-1} . Anal. Calcd for $\text{C}_{11}\text{H}_{10}\text{F}_{12}\text{O}_4$ (434.31): C, 30.43; H, 2.32. Found: C, 30.29; H, 2.21.

X-ray structural data of **5a** (CCDC 798769): water-free crystals of **5a**, suitable for X-ray crystallography, obtained by sublimation at 50 °C

under vacuum (10^{-2} mbar) in a sealed tube and through a layer of 4 Å molecular sieves, $\text{C}_{11}\text{H}_{10}\text{F}_{12}\text{O}_4$, formula weight 434.31, crystal size $0.20 \times 0.20 \times 0.10$ mm, crystal system orthorhombic, space group $P2_12_12_1$, unit cell dimensions $a = 9.9444(5)$ Å, $b = 13.0012(7)$ Å, $c = 36.1469(3)$ Å, $Z = 12$, $D_{\text{calcd}} 1.851$ g cm^{-3} , absorption coefficient 0.226 mm^{-1} , wavelength 0.71073 Å, $T = 100(2)$ K, $2\theta_{\text{max}} = 27.00^\circ$, 18 993/9372 collected/unique reflections ($R(\text{int}) = 0.05565$), final R indices ($I > 2\sigma(I)$) $R = 0.0437$, $R_w = 0.0661$, largest diff peak and hole 0.305 and -0.325 $\text{e} \text{Å}^{-3}$.

4.3.2. (4R,5R)-5-(1,1,1,3,3,3-Hexafluoro-2-hydroxypropan-2-yl)-2,2-dimethyl-1,3-dioxolane-4-carboxylic Acid (8). Analogously, 0.43 g (1.92 mmol, 1.00 equiv) of the acid chloride **7** was reacted with 1.16 mL (7.68 mmol, 5.00 equiv) of $\text{CF}_3\text{-TMS}$ (**6**) and 0.72 g (7.68 mmol, 5.00 equiv) of TMAF.

Colorless crystals (200 mg, 33%) were obtained by crystallization from DCM: mp 70–72 °C. ^1H NMR (300.1 MHz, CDCl_3): δ 11.0 (s; 1H, OH), 6.45 (s; 1H, OH), 4.78 (d; 1H, $^3J = 7.0$ Hz), 4.77 (d; 1H, $^3J = 7.0$ Hz), 1.47 (s; 3H), 1.56 (s; 3H). ^{13}C NMR (75.5 MHz, CDCl_3): δ 174.8, 120.1, 116.4, 113.7, 76.9, 76.5, 76.2, 26.1, 25.8. ^{19}F NMR (282.4 MHz, CDCl_3): δ 72.88 (q; 3F, $^4J_{\text{FF}} = 9.1$ Hz), 75.96 (q; 3F, $^4J_{\text{FF}} = 9.1$ Hz). GCMS: $\tau_R = 10.13$ min; m/z 298, 297, 267, 251, 227, 169, 145, 128, 97, 91, 85, 78, 69, 59, 55; Macherey Optima-5MS; 35 °C, 5 min, 20 °C/min \rightarrow 280 °C, 10 min. ESI-MS (neg): m/z (%) 311 [M-H^+] (99). HRMS (ESI): calcd. for $\text{C}_9\text{H}_{10}\text{F}_6\text{O}_5$ (anion): 311.03487; found: 311.03543 (error < 2 ppm). IR: $\tilde{\nu}$ = 3325 (br), 2999 (w), 2359 (w), 2332 (w), 1836 (w), 1734 (m) 1628 (w), 145 (w), 1379 (w), 1361 (w), 1210 (s), 1148 (s), 1082 (s) 1034 (w), 978 (w), 959 (w), 866 (w), 799 (w), 719 (w), 685 (w), 654 (w) cm^{-1} .

X-ray structural data of **8** (CCDC 866491): $\text{C}_9\text{H}_{10}\text{F}_6\text{O}_5$, formula weight 312.16, crystal size $0.15 \times 0.15 \times 0.02$ mm, crystal system monoclinic, space group $P2_1$, unit cell dimensions $a = 9.47(2)$ Å, $b = 6.580(10)$ Å, $c = 10.22(3)$ Å, $\beta = 106.01(6)^\circ$, $Z = 2$, $D_{\text{calcd}} 1.695$ g cm^{-3} , absorption coefficient 0.190 mm^{-1} , wavelength 0.71073 Å, $T = 100(2)$ K, $2\theta_{\text{max}} = 24.99^\circ$, 1282/1094 collected/unique reflections ($R(\text{int}) = 0.0519$), final R indices ($I > 2\sigma(I)$) $R = 0.0568$, $R_w = 0.1200$, largest diff peak and hole 0.196 and -0.215 $\text{e} \text{Å}^{-3}$.

4.4. General Procedure for the Preparation of the TEFDDOLS ($\alpha,\alpha,\alpha',\alpha'$ -tetrakis(perfluoroalkyl/aryl)-2,2'-dimethyl-1-3-dioxolane-4,5-dimethanols) 5b–f by Halogen–Lithium Exchange. (*R,R*)-Isopropylidene tartaric dichloride (**7**; 500 mg, 2.2 mmol, 1.00 equiv) and the perfluorinated alkyl/aryl iodide or bromide (7.10 equiv, 15.6 mmol) were dissolved in 30 mL of dry diethyl ether at -78 °C, and methyllithium, stabilized with lithium bromide (1.5 M in diethyl ether, 7.33 mL, 11.00 mmol, 5.00 equiv), was slowly added. The reaction mixture was stirred for 1 h at -78 °C and subsequently quenched by addition of saturated aqueous NH_4Cl (30 mL). The layers were separated, and the aqueous phase was extracted with diethyl ether. The combined organic phases were dried over MgSO_4 , and the solvent was evaporated in vacuo. The crude product (yellowish brown oil) was purified by flash chromatography (cyclohexane/EtOAc 1/1) and subsequent sublimation or crystallization to give the tetrakis(perfluoroalkyl/aryl) TEFDDOL as colorless crystals.

4.4.1. (4R,5R)-2,2-Dimethyl-4,5-bis[bis(perfluoroethyl)-hydroxymethyl]-1,3-dioxolane (5b). Pentafluoroethyl iodide was used; colorless crystals (767 mg, 55%) of the product **5b** were obtained by sublimation (10^{-2} mbar, 50 °C): mp 81–82 °C. $[\alpha]_D^{20} = +4.1^\circ$ (c 1.0, CHCl_3). ^1H NMR (300.1 MHz, CDCl_3): δ 4.86 (s; 2H), 1.44 (s; 6H), OH not detected. ^{13}C NMR (75.5 MHz, CDCl_3): δ 118.2, 118.3, 114.1, 119.9, 112.1, 78.1, 76.2, 25.8. ^{19}F NMR (282.4 MHz, CDCl_3): δ -78.56 (dd; $^3J_{\text{FF}} = 16$ Hz, $^3J_{\text{FF}} = 16$ Hz, 6F, $F-2_A''$), -78.96 (dd; $^3J_{\text{FF}} = 2.5$ Hz, $^3J_{\text{FF}} = 2.9$ Hz, 6F, $F-2_B''$), 113.08 (m; $^2J_{\text{FF}} = 290$ Hz, $^3J_{\text{FF}} = 2.5$ Hz, $^4J_{\text{FF}} = 6.7$ Hz, $^4J_{\text{FF}} = 6.7$ Hz, 2F, $F-1_B''$), -114.32 (m; $^2J_{\text{FF}} = 290$ Hz, $^3J_{\text{FF}} = 2.9$ Hz, $^4J_{\text{FF}} = 12$ Hz, $^4J_{\text{FF}} = 12$ Hz, 2F, $F-1_E''$), -118.14 (m; $^2J_{\text{FF}} = 150$ Hz, $^3J_{\text{FF}} = 16$ Hz, $^4J_{\text{FF}} = 12$ Hz, $^4J_{\text{FF}} = 6.7$ Hz, 2F, $F-1_A''$), 118.26 (m; $^2J_{\text{FF}} = 150$ Hz, $^3J_{\text{FF}} = 16$ Hz, $^4J_{\text{FF}} = 12$ Hz, $^4J_{\text{FF}} = 6.7$ Hz, 2F, $F-1_A''$). GCMS: $\tau_R = 4.13$ min; m/z 516, 499, 367, 219, 171, 147, 119, 109, 85, 69, 59; Macherey Optima-5MS; 35 °C, 5 min, 20 °C/min \rightarrow 280 °C, 10 min. ESI-MS (neg): m/z (%) 633 [$\text{M} - \text{H}^+$] (99). IR: $\tilde{\nu}$ 3390 (br), 2920 (w), 1381 (w), 1327 (w), 1306

4.5. Crystallization of the 2/1 5a/Water Complex. This hemihydrate was obtained when the TEFDDOL **5a** was crystallized from nondried DCM.

X-ray structural data of the 2/1 **5a**/water complex (CCDC 827663): $2(\text{C}_{11}\text{H}_{10}\text{F}_{10}\text{O}_4) \cdot \text{H}_2\text{O}$, formula weight 886.40, crystal size $0.20 \times 0.20 \times 0.03$ mm, crystal system monoclinic, space group $P2_1$, unit cell dimensions $a = 15.6960(7)$, $b = 12.2229(4)$ Å, $c = 17.2068(5)$ Å, $\beta = 105.3780(10)^\circ$, $Z = 4$, $D_{\text{calcd}} 1.850 \text{ g cm}^{-3}$, absorption coefficient 0.226 mm^{-1} , wavelength $0.710 73$ Å, $T = 100(2)$ K, $2\theta_{\text{max}} = 27.00^\circ$, 20 898/7274 collected/unique reflections ($R(\text{int}) = 0.0331$), final R indices ($I > 2\sigma(I)$) $R = 0.0312$, $R_w = 0.0649$, largest diff peak and hole 0.447 and $-0.337 \text{ e \AA}^{-3}$.

4.6. Crystallization of the 2/1 5b/Water Complex. This hemihydrate was obtained when the TEFDDOL **5b** was crystallized from nondried DCM.

X-ray structural data of the 2/1 **5b**/water complex (CCDC 827659): $2(\text{C}_{15}\text{H}_{10}\text{F}_{20}\text{O}_4) \cdot \text{H}_2\text{O}$, formula weight 1286.48, crystal size $0.30 \times 0.20 \times 0.10$ mm, crystal system monoclinic, space group $P2_1$, unit cell dimensions $a = 8.1163(4)$ Å, $b = 21.2609(10)$ Å, $c = 12.7665(3)$ Å, $\beta = 102.562(3)^\circ$, $Z = 2$, $D_{\text{calcd}} 1.987 \text{ g cm}^{-3}$, absorption coefficient 0.252 mm^{-1} , wavelength $0.710 73$ Å, $T = 100(2)$ K, $2\theta_{\text{max}} = 27.00^\circ$, 11 214/4791 collected/unique reflections ($R(\text{int}) = 0.0320$), final R indices ($I > 2\sigma(I)$) $R = 0.0305$, $R_w = 0.0484$, largest diff peak and hole 0.263 and $-0.222 \text{ e \AA}^{-3}$.

4.7. Crystallization of the 2/1 5b/DABCO Complex. This complex was obtained when a 1/1 mixture of TEFDDOL **5b** and DABCO was crystallized from dry DCM.

X-ray structural data of the 2/1 **5b**-DABCO complex (CCDC 827658): $2(\text{C}_{15}\text{H}_{10}\text{F}_{20}\text{O}_4) \cdot \text{C}_6\text{H}_{12}\text{N}_2$, formula weight 1380.64, crystal size $0.15 \times 0.10 \times 0.03$ mm, crystal system orthorhombic, space group $P2_12_12_1$, unit cell dimensions $a = 10.2080(6)$ Å, $b = 15.1118(10)$ Å, $c = 32.159(2)$ Å, $Z = 4$, $D_{\text{calcd}} 1.849 \text{ g cm}^{-3}$, absorption coefficient 0.225 mm^{-1} , wavelength $0.710 73$ Å, $T = 100(2)$ K, $2\theta_{\text{max}} = 27.00^\circ$, 19 818/6004 collected/unique reflections ($R(\text{int}) = 0.0815$), final R indices ($I > 2\sigma(I)$) $R = 0.0611$, $R_w = 0.1612$, largest diff peak and hole 1.048 and $-0.602 \text{ e \AA}^{-3}$.

4.8. Crystallization of the 2/3 5f/DABCO Complex. This complex was obtained when a 1/1 mixture of TEFDDOL **5f** and DABCO was crystallized from dry DCM.

X-ray structural data of the 2/3 **5f**/DABCO complex (CCDC 827656): $2(\text{C}_{31}\text{H}_{10}\text{F}_{20}\text{O}_4) \cdot 3(\text{C}_6\text{H}_{12}\text{N}_2)$, formula weight 1989.31, crystal size $0.30 \times 0.20 \times 0.10$ mm, crystal system monoclinic, space group $P2_1$, unit cell dimensions $a = 11.0460(2)$ Å, $b = 19.7743(3)$ Å, $c = 18.3995(3)$ Å, $\beta = 91.3656(7)^\circ$, $Z = 2$, $D_{\text{calcd}} 1.644 \text{ g cm}^{-3}$, absorption coefficient 0.169 mm^{-1} , wavelength $0.710 73$ Å, $T = 100(2)$ K, $2\theta_{\text{max}} = 27.00^\circ$, 9028/7567 collected/unique reflections ($R(\text{int}) = 0.0386$), final R indices ($I > 2\sigma(I)$) $R = 0.0394$, $R_w = 0.1038$, largest diff peak and hole 0.755 and $-0.46 4 \text{ e \AA}^{-3}$.

4.9. Crystallization of the 1/2 5f/Piperidine Complex. This complex was obtained when the TEFDDOL **5f** was crystallized from dry DCM in the presence of excess piperidine.

X-ray structural data of the 1/2 **5f**-piperidine complex (CCDC 827657): $(\text{C}_{31}\text{H}_{10}\text{F}_{20}\text{O}_4) \cdot 2(\text{C}_5\text{H}_{11}\text{N})$, formula weight 996.69, crystal size $0.40 \times 0.20 \times 0.10$ mm, crystal system orthorhombic, space group $P2_12_12_1$, unit cell dimensions $a = 10.3791(4)$ Å, $b = 19.8080(16)$ Å, $c = 20.2096(15)$ Å, $Z = 4$, $D_{\text{calcd}} 1.593 \text{ g cm}^{-3}$, absorption coefficient 0.163 mm^{-1} , wavelength $0.710 73$ Å, $T = 100(2)$ K, $2\theta_{\text{max}} = 27.00^\circ$, 17 925/5046 collected/unique reflections ($R(\text{int}) = 0.0588$), final R indices ($I > 2\sigma(I)$) $R = 0.0410$, $R_w = 0.0768$, largest diff peak and hole 0.254 and $-0.250 \text{ e \AA}^{-3}$.

4.10. Synthesis of (3aR,5R,6S,6aR)-2,2-dimethyl-3a,5-bis-(perfluoroethyl)tetrahydrofuro[2,3-d][1,3]dioxole-5,6-diol (rac-11). According to the general procedure given in section 4.4, 500 mg of the *meso*-anhydride **10** was reacted. Flash chromatography (EtOAc) afforded colorless crystals (640 mg, 54%) of the product *rac*-**11**: mp 118–120 °C. $^1\text{H NMR}$ (300.1 MHz, CDCl_3): δ 4.67 (br s; 1H), 4.63 (br s; 1H), 3.32 (s; 2H, OH), 1.50 (s; 3H), 1.37 (s; 3H). $^{13}\text{C NMR}$ (75.5 MHz, CDCl_3): δ 120.3–120.6, 119.5, 112.8, 108.9, 79.2, 74.3, 25.3, 23.7. $^{19}\text{F NMR}$ (282.4 MHz, CDCl_3): δ -79.81 (d; 3F, $^3J_{\text{FF}} = 14.0$ Hz), -79.22 (dd; 3F, $^3J_{\text{FF}} = 14.4$, 6.4 Hz), -114.63–

119.05 (m; 4F). GCMS: $t_{\text{R}} = 9.81$ min; m/z 380, 379, 347, 315, 289, 267, 247, 219, 201, 185, 171, 145, 133, 119, 100, 85, 69, 59; Macherey Optima-5MS; 35 °C, 5 min, 20 °C/min \rightarrow 280 °C, 10 min. ESI-MS (neg): m/z (%) 411 [$\text{M} - \text{H}^+$] (99). IR: $\tilde{\nu}$ 3676 (w), 3402 (br), 2988 (w), 2901 (w), 1624 (w), 1451 (w), 1383 (w), 1329 (w), 1177 (m), 1076 (m), 974 (w), 878 (w), 802 (w), 727 (w) cm^{-1} . HRMS (ESI-): calcd for $\text{C}_{11}\text{H}_{10}\text{F}_{10}\text{O}_5$ (anion) 411.028 48, found 411.028 60 (error < 1 ppm).

X-ray structural data of *rac*-**11** (CCDC 827665): $\text{C}_{11}\text{H}_{10}\text{F}_{10}\text{O}_5$, formula weight 412.19, crystal size $0.15 \times 0.07 \times 0.01$ mm, crystal system monoclinic, space group $P2_1/c$, unit cell dimensions $a = 5.4658(2)$ Å, $b = 17.8420(12)$ Å, $c = 15.3081(3)$ Å, $\beta = 104.041(3)^\circ$, $Z = 4$, $D_{\text{calcd}} 1.890 \text{ g cm}^{-3}$, absorption coefficient 0.224 mm^{-1} , wavelength $0.710 73$ Å, $T = 100(2)$ K, $2\theta_{\text{max}} = 27.00^\circ$, 7359/3140 collected/unique reflections ($R(\text{int}) = 0.0354$), final R indices ($I > 2\sigma(I)$) $R = 0.0360$, $R_w = 0.0538$, largest diff peak and hole 0.295 and $-0.278 \text{ e \AA}^{-3}$.

■ ASSOCIATED CONTENT

Supporting Information

NOESY-spectra and DOSY-data of the TEFDDOLs **5b,f**; CIF files, ORTEP drawings and crystallographic data for all X-ray structures determined in this paper. This material is available free of charge via the Internet at <http://pubs.acs.org>. The CCDC numbers stated in section 4 also contain supplementary crystallographic data for this paper. These data can be obtained free of charge from The Cambridge Crystallographic Data Centre via www.ccdc.cam.ac.uk/data_request/cif.

■ AUTHOR INFORMATION

Corresponding Author

*E-mail: berkessel@uni-koeln.de. Fax: (+49) 221-4705102.

Notes

The authors declare no competing financial interest.

■ ACKNOWLEDGMENTS

Financial support by the Deutsche Forschungsgemeinschaft DFG (Priority Program 1179, "Organocatalysis") and by the Fonds der Chemischen Industrie is gratefully acknowledged.

■ REFERENCES

- (1) (a) Pihko, P., Ed. *Hydrogen Bonding in Organic Synthesis*; Wiley-VCH: Weinheim, Germany, 2009. (b) Berkessel, A.; Gröger, H. *Asymmetric Organocatalysis*, Wiley-VCH: Weinheim, Germany, 2005. (c) Dalko, P. I., Ed. *Enantioselective Organocatalysis*, Wiley-VCH: Weinheim, Germany, 2007. (d) List, B.; Yang, J. W. *Science* **2006**, *313*, 1584–1586. (e) Melchiorre, P.; Marigo, M.; Carlone, A.; Bartoli, G. *Angew. Chem., Int. Ed.* **2008**, *47*, 6138–6171.
- (2) (a) Kotke, M.; Schreiner, P. R. In *Hydrogen Bonding in Organic Synthesis*; Pihko, P., Ed.; Wiley-VCH: Weinheim, Germany, 2009; pp 141–351. (b) Zhang, Z.; Schreiner, P. R. *Chem. Soc. Rev.* **2009**, *38*, 1187–1198. (c) Connon, S. J. *Synlett* **2009**, *65*, 1219–1234. (d) Taylor, M. S.; Jacobsen, E. N. *Angew. Chem. Int. Ed.* **2006**, *45*, 1520–1543. (e) Takemoto, Y. *Org. Biomol. Chem.* **2005**, *3*, 4299–4306.
- (3) Aleman, J.; Parra, A.; Jiang, H.; Jørgensen, K. A. *Chem. Eur. J.* **2011**, *17*, 6890–6899. (b) Amendola, V.; Fabbrizzi, L.; Mosca, L. *Chem. Soc. Rev.* **2010**, *39*, 3889–3915. (c) Malerich, J. P.; Hagihara, K.; Rawal, V. H. *J. Am. Chem. Soc.* **2008**, *130*, 14416–14417.
- (4) (a) Gondi, V. B.; Hagihara, K.; Rawal, V. H. *Chem. Commun.* **2010**, 904–906. (b) Villano, R.; Acocella, M. R.; Massa, A.; Palombi, L.; Scettri, A. *Tetrahedron* **2009**, *65*, 5571–5576. (c) Huang, Y.; Unni, A. K.; Thadani, A. N.; Rawal, V. H. *Nature* **2003**, *424*, 146.
- (5) (a) Seebach, D.; Beck, A. K.; Heckel, A. *Angew. Chem., Int. Ed.* **2001**, *40*, 92–138. (b) Beck, A. K.; Bastani, B.; Plattner, D. A.; Petter, W.; Seebach, D.; Braunschweiger, H.; Gysi, P.; La Vecchia, L. *Chimia*

1991, 45, 238–244. (c) Berkessel, A.; Etzenbach-Effers, K. In *Hydrogen Bonding in Organic Synthesis*; Pihko, P., Ed.; Wiley-VCH: Weinheim, Germany, 2009; pp 15–42. (d) Berkessel, A.; Etzenbach-Effers, K. *Top. Curr. Chem.* **2010**, 291, 1–27.

(6) Seebach, D.; Beck, A. K.; Bichsel, H.-U.; Pichota, A.; Sparr, C.; Wünsch, R.; Schweizer, W. B. *Helv. Chim. Acta* **2012**, 95, 1303–1324.

(7) (a) Shuklov, I. A.; Dubrovina, N. V.; Börner, A. *Synthesis* **2007**, 2925–2943. (b) Bégué, J.-P.; Bonnet-Delpon, D.; Crousse, B. *Synlett* **2004**, 18–29.

(8) Ebersson, L.; Hartshorn, M. P.; Persson, O. *J. Chem. Soc., Perkin Trans. 2* **1995**, 1735–1744.

(9) (a) Berkessel, A. In *Modern Oxidation Methods*, 2nd ed.; Bäckvall, J. E., Ed.; Wiley-VCH: Weinheim, Germany, 2010; pp 117–145.

(b) Legros, J.; Crousse, B.; Bonnet-Delpon, D.; Bégué, J.-P. *Tetrahedron* **2002**, 58, 3993–3998.

(10) (a) Berkessel, A.; Adrio, J.; Hüttenhain, D.; Neudörfl, J. M. *J. Am. Chem. Soc.* **2006**, 128, 8421–8424. (b) Berkessel, A.; Adrio, J. *J. Am. Chem. Soc.* **2006**, 128, 13412–13420.

(11) Christ, P.; Lindsay, A. G.; Vormittag, S. S.; Neudörfl, J.-M.; Berkessel, A.; O'Donoghue, A. C. *Chem. Eur. J.* **2011**, 17, 8524–8528.

(12) (a) Terada, M. *Curr. Org. Chem.* **2011**, 15, 2227–2256. (b) Rueping, M.; Nachtsheim, B. J.; Ieawsuwan, W.; Atodiresei, I. *Angew. Chem., Int. Ed.* **2011**, 50, 6706–6720. (c) Yamamoto, H.; Cheon, C. H. In *Catalytic Asymmetric Synthesis*, 3rd ed.; Ojima, I., Ed.; Wiley: Hoboken, NJ, 2010; pp 119–161. (d) Kampen, D.; Reisinger, C. M.; List, B. *Top. Curr. Chem.* **2010**, 291, 395–456. (e) Akiyama, T.; Itoh, J.; Fuchibe, K. *Adv. Synth. Catal.* **2006**, 348, 999–1010.

(13) Burton, D. J.; Yang, Z.-Y. *Tetrahedron* **1992**, 48, 189–275.

(14) (a) Ruppert, I.; Schlich, K.; Volbach, W. *Tetrahedron Lett.* **1984**, 25, 2195–2198. (b) Surya Prakash, G. K.; Yudin, A. K. *Chem. Rev.* **1997**, 97, 757–786.

(15) Hafner, A.; Duthaler, R.; Marti, R.; Rihs, G.; Rothe-Streit, P.; Schwarzenbach, F. *J. Am. Chem. Soc.* **1992**, 114, 2321–2336.

(16) El Sheikh, S.; Schmalz, H.-G. *Drug Disc. Devel.* **2004**, 7, 882–895.

(17) Delaney, E. J.; Massil, S. E.; Shi, G.-Y.; Klotz, I. M. *Arch. Biochem. Biophys.* **1984**, 228, 627–638.

(18) (a) Babadzhanova, L. A.; Kirij, N. V.; Yagupolskii, Y. L.; Tyrta, W.; Naumann, D. *Tetrahedron* **2005**, 61, 1813–1819. (b) For the addition of Ruppert's reagent to tartaric acid derived 1,4-diketones, see: Harakat, D.; Massicot, F.; Nonnenmacher, J.; Grellepois, F.; Portella, C. *Chem. Eur. J.* **2011**, 17, 10636–10642.

(19) Takemura, H.; Kaneko, M.; Sako, K.; Iwanaga, T. *New J. Chem.* **2009**, 33, 2004–2006.

(20) (a) Irurre, J.; Alonso-Alija, C.; Piniella, J. F.; Alvarez-Larena, A. *Tetrahedron: Asymmetry* **1992**, 3, 1591–1596. (b) Gerard, B.; Sangji, S.; O'Leary, D. J.; Porco, J. A., Jr. *J. Am. Chem. Soc.* **2006**, 128, 7754–7755.

(21) Dunitz, J. D.; Taylor, R. *Chem. Eur. J.* **1997**, 3, 89–98.

(22) Schneider, H.-J. *Chem. Sci.* **2012**, 3, 1381–1394.

(23) Benoit, R. L.; Lefebvre, D.; Fréchette, M. *Can. J. Chem.* **1987**, 65, 996–1001.

(24) Crampton, M. R.; Robotham, I. A. *J. Chem. Res.* **1997**, 22–23.

(25) Cabrita, E. J.; Berger, S. *Magn. Reson. Chem.* **2001**, 39, S142–S148.

(26) Armarego, A. L. F.; Chai, C. L. L. *Purification of Laboratory Chemicals*, 5th ed.; Butterworth-Heinemann: London, 2003.

(27) Bauer, W. *Magn. Reson. Chem.* **1996**, 34, 532–537.

(28) Martin, J. S.; Quirt, A. R. *J. Magn. Reson.* **1971**, 5, 318–327 (modified by R. Sebastian).

(29) (a) Suhm, M. A. *Adv. Chem. Phys.* **2009**, 142, 1–57. (b) Schaal, H.; Häber, T.; Suhm, M. A. *J. Phys. Chem. A* **2000**, 104, 265–274.